Nuclear Physics **A500** (1989) 287–300
North-Holland, Amsterdam

BETA-DELAYED PROTON DECAY OF ^{28}S*

F. POUGHEON, V. BORREL and J.C. JACMART

Institut de Physique Nucléaire, BP no. 1, 91406 Orsay, France

R. ANNE, C. DÉTRAZ, D. GUILLEMAUD-MUELLER[1] and A.C. MUELLER[1]

GANIL, BP 5027, 14021 Caen, France

D. BAZIN, R. DEL MORAL, J.P. DUFOUR, F. HUBERT and M.S. PRAVIKOFF

CEN Bordeaux, Le Haut Vigneau, 33170 Gradignan, France

G. AUDI

CSNSM, Laboratoire René Bernas, Batiment 108, 91405 Orsay, France

E. ROECKL

GSI, Postfach 11 05 52, 6100 Darmstadt 11, Fed. Rep. Germany

B.A. BROWN

Nat. Sup. Cyclotron Lab., and Dept. of Physics and Astronomy, MSU, East Lansing, MI 48 824, USA

Received 8 February 1989
(Revised 28 March 1989)

Abstract: Beta-delayed proton radioactivity has been observed for the ^{28}S isotope ($T_z = -2$), produced by projectile fragmentation of 85 MeV/u ^{36}Ar. The measured half-life of ^{28}S is 125 ± 10 ms. Energy spectra of beta-delayed protons have been measured. The lowest $T = 2$ state in the daughter nucleus ^{28}P has been located at an excitation energy of 5900 ± 21 keV. A comparison of the experimental data to the quadratic form of the isobaric multiplet mass equation shows that the energies of the five $T = 2$ states of the $A = 28$ quintet are well represented by that relation. Shell-model predictions for the half-life of ^{28}S and the location and decay properties of the lowest $T = 2$ state of ^{28}P are in good agreement with experimental data.

E | RADIOACTIVITY ^{28}Si(β^+p) [from Ni(^{36}Ar, ^{28}S), $E = 3060$ MeV] measured beta-delayed E_p, I_p, $T_{1/2}$. ^{28}P deduced levels. Heavy-ion identification: magnetic analysis, time-of-flight measurement; solid-state detector telescope.

1. Introduction

Recent progress in studies of very proton-rich nuclides near or at the drip line has greatly been advanced by the effectiveness of intermediate-energy heavy-ion fragmentation coupled with good instrumentation techniques [1-3]).

The rapid increase of mass excess as one approaches the proton drip line along an isobar leads, through β^+ decay, to a broad range of excited states in the daughter

* Experiment performed at the GANIL National Laboratory.

[1] Present address: Institut de Physique Nucléaire, BP no. 1, 91406 Orsay, France.

0375-9474/89/$03.50

nucleus, including in particular the lowest isobaric analogue state through the super-allowed transition.

Isobaric multiplets play an important role for mass predictions. They also contribute to our understanding of charge dependent effects in nuclear forces. The masses of analogue states in an isospin multiplet are given to first order by a quadratic relationship [4])

$$M(A, T, T_z) = a(A, T) + b(A, T)T_z + c(A, T)T_z^2 .$$

This isobaric multiplet mass equation (IMME) is obtained from first-order perturbation theory with the assumption that the wave functions of the members of an isospin multiplet are identical and that only two-body forces are responsible for charge-dependent effects in nuclei. Deviations from this quadratic equation are generally represented by additional terms $d(A, T)T_z^3$ and $e(A, T)T_z^4$ in which the coefficients d and e can be derived from second-order perturbation theory. To study these deviations, isospin multiplets with $T \geqslant \frac{3}{2}$ are needed.

Extensive studies of isospin quartets have led to an excellent agreement with the quadratic form of the IMME, with only one significant deviation at $A = 9$ [5]). Whereas, most of the physical effects that could be considered are absorbed in the b and c coefficients for quartets, producing thus an almost perfect quadratic IMME, the situation is quite different in isobaric quintets, where for example isobaric spin mixing, when it exists, could produce definite non-zero additional $e(A, T)$ terms [5]).

While in 1978 only one complete quintet of states (the $A = 8$ quintet) was known [5]), nowadays, including the present work, all the $A = 4n$ lowest-lying quintets below $A = 40$ are known, with the exception of the $T_z = -1$ members at $A = 12$, 16 and 40 [6]). None of the $A = 4n + 2$ quintets is presently available; only in one case ($A = 22$) three members out of five are known [7]). Both in the $A = 4n$ and $A = 4n + 2$ nuclei these difficulties are due to the fact that up to now there is no good general method for identifying a $T = 2$ state in a $T_z = -1$ nucleus when the corresponding $T_z = -2$ isobar is unstable against particle decay [8]). In the present situation, the known full or partial (4 members) quintets show no evidence for non-zero cubic (d) or quartic (e) term, except in two cases (over eight). The $A = 8$ quintet as compiled and analysed by Benenson and Kashy in 1979 [5]) exhibited definite non-zero d- and (or) e-coefficients. In the more recent analysis by Antony *et al.* [6]), these coefficients vanish with upper limits of 5 and 4 keV respectively. The change is due to unpublished results [9]) quoted by the latter authors for the mass-excesses of the isobaric analog state $T = 2$ of ^{8}Be and ^{8}Li. This situation would benefit of clarification.

The second case is the $A = 20$ quintet for which $d = -4.0\,(1.8)$ keV and $e = -4.2\,(1.7)$ keV [ref. [6])]. In all other six cases these coefficients vanish with upper limits ranging between 2 and 8 keV at the 95% confidence level.

This context shows the need for more information on the higher order terms of the IMME in isobaric quintets, and it is one of the goals of the present work to shed more light on them through completion of the 28-mass isospin quintet.

In this paper we report on data for the β^+-delayed proton decay of ^{28}S. The β^+ decay is highly selective in populating the $T = 2$ analog state in the daughter nucleus via a super-allowed beta-decay branch.

The study of the β^+-delayed proton spectrum of ^{28}S results in the location of the lowest $T = 2$ state in the $T_z = -1$ ^{28}P daughter nucleus, allowing a test of the quadratic isobaric multiplet mass equation.

Furthermore, the half-life and β^+-decay branching ratios were determined and compared to shell-model calculations.

2. Experimental method

The GANIL accelerator delivered a 85 MeV/u ^{36}Ar beam with an electron intensity of 1 μA on a natural nickel target with a thickness of 395 mg/cm^2. The reaction products were selected using the LISE spectrometer operated as an isotope separator [10,11]). A 180 mg/cm^2 thick aluminium degrader was placed between the two dipoles. It was designed to preserve the achromatism of the spectrometer [11]).

The heavy ions emerging from LISE were implanted and identified in a six element solid-state telescope located at the final focal point of LISE (see fig. 1). The thickness of the silicon detectors were 300 μm (ΔE_1), 123 μm (E_2), 122 μm (E_3), 118 μm (E_4), 432 μm (E_5) and 5500 μm (E_6) (fig. 1).

The four detectors E_2, E_3, E_4 and E_5 were mounted as close as possible to each other in order to maximize the efficiency of the proton detection.

A 550 μm thick aluminium foil placed in front of the telescope slowed down the ions so that the ^{28}S nuclei stopped in the E_4 detector. With the momentum acceptance of LISE set by slits to $\Delta p/p = \pm 0.8\%$, all the ^{28}S ions were collected in that detector.

The experimental procedure has been described in details in a previous paper [3]). Briefly, a dual system of data acquisition is involved. A first data-acquisition system records the energy deposits of the heavy-ions in the silicon detectors and the

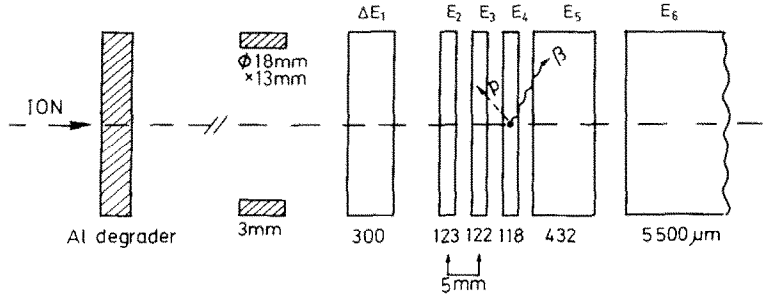

Fig. 1. The telescope of solid-state detectors. The heavy ions (^{28}S) are implanted in the E4 detector. Protons are detected in detectors E3, E4, E5. E6 is used as a veto against high-energy protons.

time-of-flight of the ions between the target and the telescope. The two-dimensional plot ΔE_1 versus time-of-flight (t.o.f.) provides a good identification of the detected nuclei. Two single-channel analysers, (ΔE_1 and t.o.f.), delivered a signal each time that a ^{28}S nuclei was identified. The beam was then stopped for a period of 250 ms, the heavy-ion data-acquisition system was disabled, and a second data acquisition was activated and its clocks started.

Since the E_2, E_3, E_4, E_5, detectors had to measure the relatively low energy of β-delayed protons a very short time after the implantation of a highly energetic ^{28}S nucleus in the detector, especially designed charge-sensitive preamplifiers were used. The amplification included two different electronic paths. The first one, devoted to the detection of the protons was equipped with a high-pulse rejection device [12]: after proper shaping, the signal was delay-line clipped and a gate rejected all pulses corresponding to heavy ions. The amplifier saturation that would have occurred from detection of the heavy ion was thus eliminated with no noticeable deterioration of the signal-to-noise ratio. The proton energies and their time of arrival were recorded by the second data-acquisition system. The heavy-ion parameters and the proton parameters were stored chronologically on the same magnetic tape.

3. Experimental results

Due to the additional selection introduced by the spectrometer when a degrader is placed at the intermediate focal plane [11]), the nuclides transmitted together with ^{28}S by the LISE separator are essentially restricted to the $N = 12$ isotones. Among these isotones, ^{27}P is a weak beta-delayed proton precursor with a proton branching ratio of $\sim 5 \times 10^{-3}$ [ref. [13])]. ^{26}Si and ^{25}Al do not emit beta-delayed particles [14]).

Some $N = 11$ isotones are also partly transmitted but have a different range. Among them, ^{25}Si is known to be a beta-delayed proton precursor [14]). With the 550 μm aluminium absorber in front of the detector, the ^{25}Si is embedded in the middle of the E_5 detector and does not contaminate the ^{28}S proton spectrum recorded in the E_4 and E_3 detectors. However it was used to calibrate the energy response of E_4 in a run with a different (680 μm thick) aluminium absorber in order to implant the ^{25}Si in the middle of E_4 detector. Its beta-delayed protons are well known [15]) and thus yield a precise proton energy calibration.

In this particular ^{28}S study, only the proton spectrum recorded in the E_4 detector was exploited since the E_5 proton spectrum was too disturbed by the ^{25}Si contamination and the E_3 detector had a poor resolution.

The energy spectrum of the β-delayed protons emitted during the beam-off time by ^{28}S implanted in the E_4 detector is displayed in fig. 2. The main peaks in this figure are assigned to the decay of ^{28}S. Since the proton energy and the recoil energy from the ion are measured in the same detector, the total decay energy (center-of-mass energy) is directly obtained. Table 1 lists the proton decay energies for the observed peaks, their relative and absolute intensities.

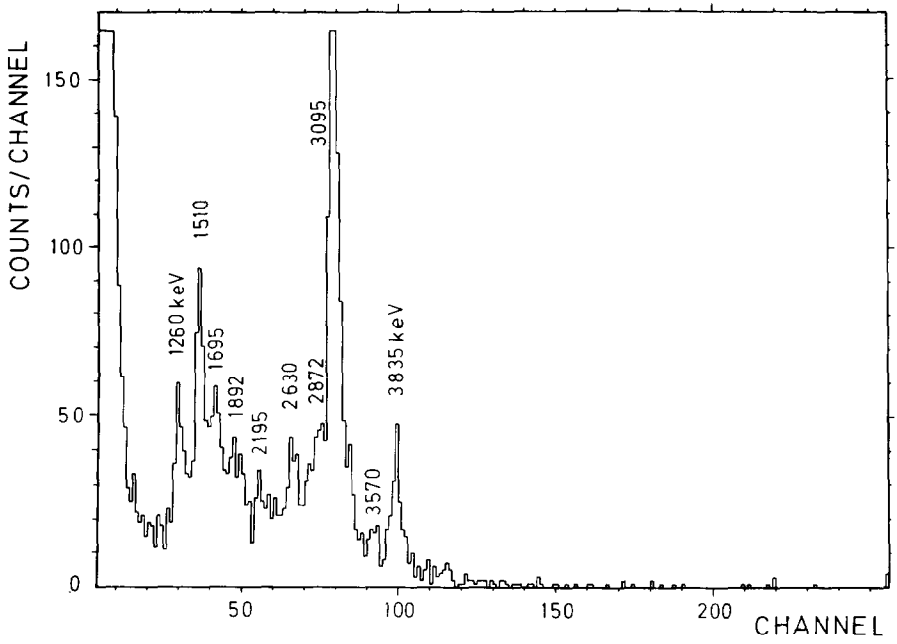

Fig. 2. Energy spectra of β-delayed protons recorded in detector E4 during 250 ms long beam-off period following the implantation of ^{28}Si ion. The detection of positron is responsible for the events below 1 MeV.

TABLE 1

Decay energies, relative and absolute intensities of β-delayed proton peaks [a])

$E_{c.m}$ keV	Relative intensity I_r (relative to 100 for the most intense peak at 3095 keV)	Absolute intensity I_p(%)
1260 ± 25	20 ± 3	1.4 ± 0.4
1510 ± 25	30 ± 5	2.1 ± 0.6
1695 ± 30	24 ± 3	1.7 ± 0.4
1892 ± 30	19 ± 3	1.3 ± 0.3
2195 ± 30	15 ± 3	1.0 ± 0.3
2630 ± 25	22 ± 3	1.6 ± 0.4
2872 ± 30	25 ± 3	1.75 ± 0.4
3095 ± 20	100	7.0 ± 1.5
3570 ± 30	13 ± 2	0.9 ± 0.2
3835 ± 20	28 ± 3	2.0 ± 0.4

[a]) See text for the uncertainties.

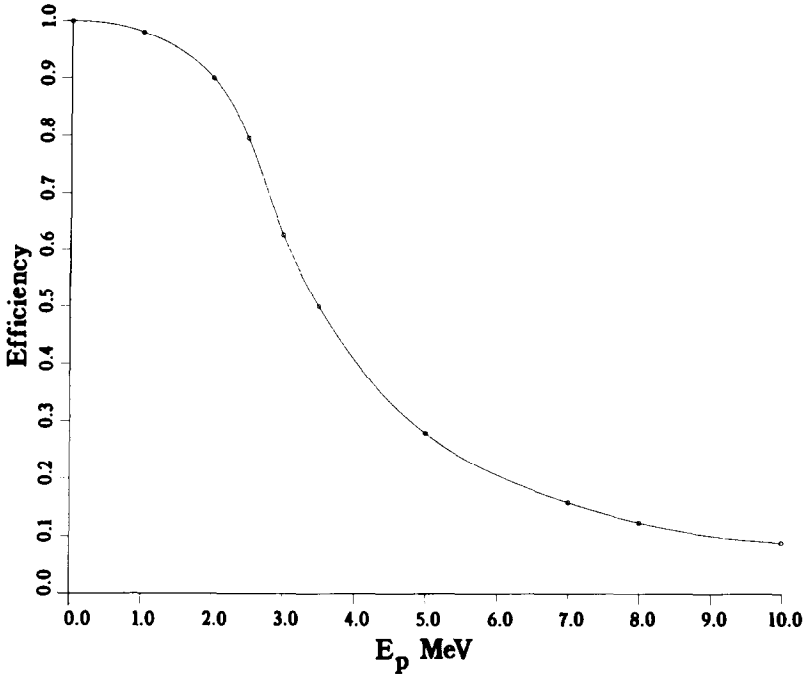

Fig. 3. Calculated efficiency of the E4 detector as a function of the proton energy. This efficiency is calculated by taking into account the energy distribution of the ^{28}S ions implanted in the E4 detector, and the geometry of the telescope.

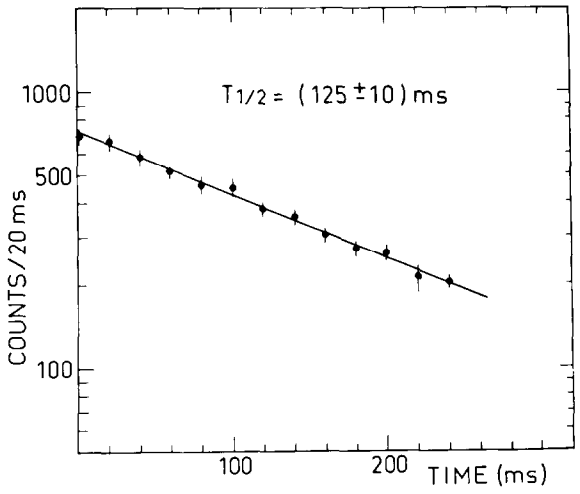

Fig. 4. Time characteristic of β-delayed proton lines assigned to the ^{28}S decay.

The uncertainties on the proton energies quoted in table 1, are obtained by quadratically adding the uncertainty of the centroid location and a calibration uncertainty of 18 keV.

The relative intensities are deduced by integrating the full-energy peaks and applying a correction factor to account for protons whose energy is only partially collected in the E_4 detector. The implantation depth profile deduced from the ^{28}S energy-loss spectrum in the E_4 detector has been taken into account for this calculation. This efficiency curve is shown in fig. 3. Absolute proton intensities are obtained by dividing the corrected number of protons by the number of ^{28}S ions embedded in the E_4 detector. The uncertainties of the intensities result from statistics, background substraction and correction factors.

The main peaks yield consistent half-life values. Fig. 4 shows the decay curve of β-delayed protons from ^{28}S summed for the main peaks. From these data, the half-life of ^{28}S is obtained as 125 ± 10 ms.

4. Discussion

For the beta-decay of ^{28}S to the isobaric analogue state in ^{28}P, under the assumption of a pure Fermi decay with no isospin mixing one obtains a reduced transition probability $B(\mathrm{F}) = 4$ and thus a $\log ft = 3.19$. Taking into account the ^{28}S measured half-life, this leads to an estimated branching ratio equal to $\sim 14\%$. No other decay leading to this energy region ($E_x \sim 6$ MeV) would be consistent with such a $\log ft$ value and such a branching ratio. It is thus clear that in the following discussion the identification of the ^{28}P $T = 2$ state is based on this argument.

We start out with a discussion of masses and IMME analysis for $A = 28$ in sects. 4.1 and 4.2. For deriving the excitation energy of the 0^+, $T = 2$ ^{28}P level from proton decay energies, spectroscopic factors are used which are described, together with an analysis of the ^{28}S decay scheme, in sect. 4.3.

4.1. TEST OF THE ISOBARIC MULTIPLET MASS EQUATION

Three of the observed proton lines can be attributed to proton emission following the super allowed β-decay of the 0^+, $T = 2$ ^{28}P level:

- 3835 keV (to ^{27}Si g.s. $\frac{5}{2}^+$ level);
- 3095 keV (to ^{27}Si 780 keV $\frac{1}{2}^+$ level);
- 2872 keV (to ^{27}Si 957 keV $\frac{3}{2}^+$ level).

Nevertheless, due to the non-ambiguity of the 3835 keV peak (see discussion in sect. 4.3), the location of the 0^+, $T = 2$ ^{28}P level is based on this peak. Its proton decay Q-value leads to a mass excess value of -1261 ± 21 keV i.e. to an excitation energy of 5900 ± 21 keV. The resulting weighted average for the three peaks would lead to a satisfactory compatible value of 5918 ± 23 keV (the ground state masses used here for ^{27}Si and ^{28}P are from ref. [16]).

TABLE 2

Properties of the $T = 2$ levels which are members of the isospin quintet at mass 28

Nucleus	T_z	Mass excess (keV)	Ref.	E_x (keV)	Ref.
^{28}S	−2	4073 ± 160 [a])	[17])	g.s.	
^{28}P	−1	−1261 ± 21	this work	5900 ± 21	
^{28}Si	0	−6268.2 ± 2.6	[20,21])	15 224.7 ± 2.7	
^{28}Al	+1	−10 858.6 ± 0.7		5992.4 ± 0.4	[22])
^{28}Mg	+2	−15 019.2 ± 2.1	[23])	g.s.	

[a]) See text for this recalibrated value.

The identification of the $T = -2$ level completes, for the first time, the isospin quintet for mass $A = 28$. Table 2 summarizes and updates the present knowledge of the properties of the members of this isospin quintet.

The ground-state mass of the $T_z = -2$ member, ^{28}S, has been determined to be 4134 ± 160 keV by Morris *et al.* [17]) in a pion double-charge-exchange reaction on ^{28}Si. The published Q-value was calibrated with the ^{26}O(π^+, π^-)^{16}Ne reaction as obtained by the same group two years earlier [18]). More recent and more precise measurement of the ^{16}Ne mass in the ^{20}Ne(α, ^{8}He)^{16}Ne reaction [19]) shows that a recalibration is necessary, giving thus a mass excess of 4073 ± 160 keV for the ground state of ^{28}S.

For the $T_z = 0$ member, ^{28}Si, we have averaged the two values $E_x = 6115$ (3) keV [ref. [20])] and $E_x = 6117$ (5) keV [ref. [21])] obtained for the alpha resonance energy in ^{24}Mg + α, using the masses of ^{24}Mg + α and ^{28}Si from the most recent atomic mass table [ref. [16])]. The excitation energy of the $T = 2$ level in the $T_z = +1$ member, ^{28}Al, is very accurately known [22]) and, when combined with the g.s. mass excess [16]) gives a value for ^{28}Al (I.A.S.) with a precision of 0.7 keV. The ground state mass of the $T_z = +2$ member, ^{28}Mg is derived from the Q_β measurement of Olsen *et al.* [23]) to the 1372.8 keV level in ^{28}Al.

The coefficients in the IMME derived from three-, four-, and five-parameter fit to the masses from table 2 are presented in table 3. In order to check the validity of the isobaric multiplet mass equation, the normalized χ^2_ν is also given. An excellent fit ($\chi^2_\nu = 0.48$) is obtained by using the purely quadratic IMME.

Higher order fits set upper limits independently on the third- and fourth-order term d and e of 7 and 4 keV, respectively, at the 95% confidence level in the $T = 2$ quintet at mass 28. The "significance" [24]) or quantity of information brought by the present work on ^{28}P is 79% in the determination of the d-coefficient and 94% in the determination of e.

This result ascertains the insignificance of charge-dependent mixing which confirms the results obtained in the $A = 20$, 24 and 36 mass [25,26]).

TABLE 3

Coefficients (in keV) and the χ^2 of the different adjustments of the isobaric multiplet mass equation for the $A = 28$ quintet parametrized as $M = a + bT_z + cT_z^2 + dT_z^3 + eT_z^4$

a	b	c	d	e	χ^2_ν [a])
-6268.9 ± 2.4	-4804.0 ± 4.0	214.4 ± 1.7			0.48
-6268.1 ± 2.6	-4799.6 ± 6.4	206.1 ± 9.4	2.9 ± 3.3		0.17
-6268.2 ± 2.6	-4797.0 ± 10.0	205.2 ± 12.1		1.4 ± 1.8	0.38
-6268.2 ± 2.6	-4807.1 ± 19.1	211.3 ± 15.6	8.5 ± 13.8	-3.1 ± 7.5	

[a]) Reduced $\chi^2_\nu = \chi^2/\nu$ where ν is the number of degrees of freedom.

Thus the overall results with quintets $A \geq 20$ indicate no necessity for the introduction of d- and e-coefficients and support the validity of the simple quadratic mass equation.

4.2. MASS OF ^{28}S

We can start from the now more steady assumption of a purely quadratic IMME to derive the mass-excess value of the ^{28}S g.s. The best fit to the four last members in table 2 thus yields a value of 4198 ± 16 keV for ^{28}S with a χ^2_ν of 0.38. This result is in good agreement with another IMME prediction of 4205 ± 16 keV [ref. [6])] and also with the experimental value of 4073 ± 160 keV from the above mentioned recalibration of the result obtained by Morris *et al.* [17]).

According to these authors, the uncertainty in their mass measurement reflects the poor resolution due to target thickness. We want to point out that remeasurement of the mass of ^{28}S in the same reaction with optimal experimental conditions or alternatively in a (α, ^{8}He) reaction [19]) would provide very valuable information. Simulation of IMME under the assumption of a 50 keV uncertainty on the mass of ^{28}S indicates that the d- and e-coefficients could be obtained with precisions of 2 and 1.5 keV, respectively. This would lead to corresponding increase of significance [24]) of such measurement from 21% presently to 74% in the determination of the d coefficient and from 6% to 41% for e.

4.3. DECAY SCHEME AND COMPARISON WITH SHELL-MODEL PREDICTIONS

From these experimental results, supported by theoretical predictions, a partial decay scheme is proposed for ^{28}S (see fig. 5). The measured g.s. mass-excess value of -7161 ± 4 keV for ^{28}P [ref. [16])] and of 4073 ± 160 keV for ^{28}S [ref. [17])] yield a Q_{EC} value $11\,234 \pm 160$ keV for the ^{28}S decay.

In table 4 we show the proton-decay energies expected from levels observed with $l = 0$ transfer in a recent ^{28}Si(p, n)^{28}P experiment [27]). The $l = 0$ transfer selected out

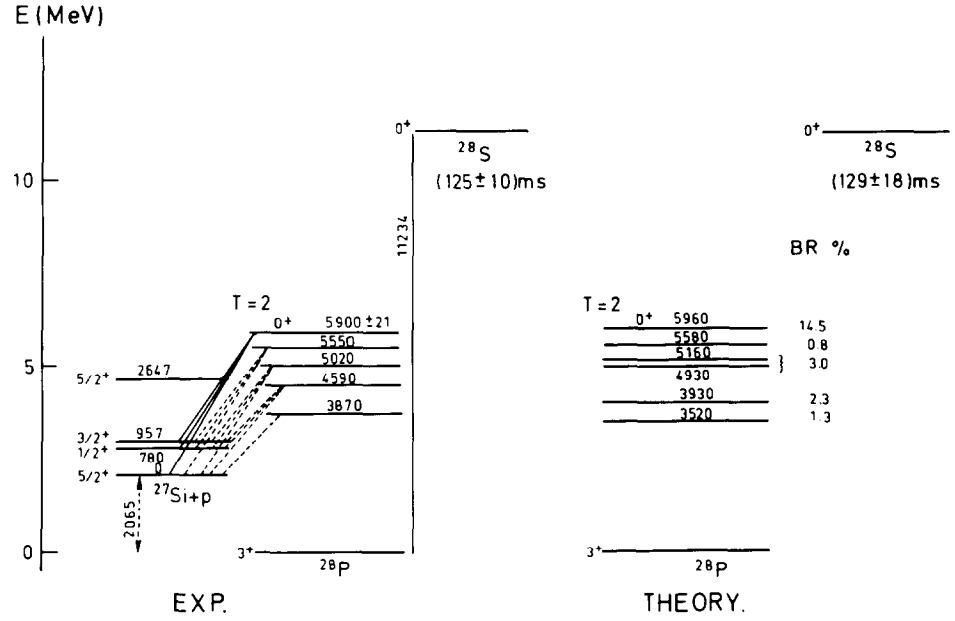

Fig. 5. Partial decay scheme of ^{28}S. For the ^{28}P nucleus, the levels are taken from the ^{28}Si(p, n)^{28}P data [27]) with the exception of the $T = 2$ state deduced from this work. Only the ^{28}P levels above 3 MeV have been indicated. Energies are in keV. The theoretical predictions are also presented.

TABLE 4

States observed in the ^{28}Si(p, n)^{28}P reaction with $l = 0$ (below 8 MeV in excitation) and the expected proton energies above the experimental threshold of 1.1 MeV for the decay to low-lying states in ^{27}Si. Deduced branching ratios (BR) are compared to theory

E_x(p, n) (MeV) [a])	Expected proton-decay energy (MeV)			Deduced beta-decay BR (%)		Predicted	
	p_0	p_1	p_2	min	max	E_x (MeV)	BR (%)
1.25						1.36	46.5
1.59						1.75	8.0
2.10						2.07	20.7
2.94						3.20	1.2
3.87	1.81 [b])			0	3.0	3.52	1.3
4.59	2.53 [b])	1.75 [b])	1.57 [b])	2	5.0	3.93	2.3
5.02	2.96 [b])	2.18 [b])	2.00 [b])	1.0	4.0	4.93+5.16	3.0
5.55	3.49 [b])	2.71 [b])	2.53 [b])	0.9	3.9	5.58	0.8
5.91	3.85 [b])	3.07 [b])	2.89 [b])	2	10.8±2.4	5.96	14.5
6.50	4.44	3.66	3.48			>6	2.2

[a]) B.D. Anderson *et al.* [27]). The errors are about 0.1 MeV.

[b]) Energies which correspond to within 0.1 MeV with observed proton decay energies.

the 0^+ and 1^+ states in ^{28}P. The level observed at 5.91 MeV in (p, n) is consistent with our energy for the 0^+, $T=2$ state. This $T=0$ to $T=2$ transition is forbidden in (p, n) for states with good isospin and assuming a direct one-step reaction, but it could be seen due to isospin mixing and/or a two-step reaction process. Also, there could be a $1^+(T=1)$ state at the same energy.

All of the proton energies observed in beta decay (except for the 1.26 MeV proton peak) correspond nicely with those expected from the decay of levels observed in (p, n) to the $\frac{5}{2}^+$ ground state (p_0), $\frac{1}{2}^+$ first excited state (p_1) or $\frac{3}{2}^+$ second excited state (p_2) of ^{27}Si. It is clear, however, that there is some ambiguity in these assignments and that often one proton peak can be assigned to different decays. The beta-decay branching ratios calculated with the wave functions of Wildenthal [28]) and the effective Gamow-Teller operator from ref. [29]) are given in table 4. The phase-space factors were calculated as in ref. [29]) using the Q_{EC} value calculated above.

These predictions are compared with the branching ratios deduced from the matchups between the energies in table 1 and those indicated in table 4. When an ambiguity exists in the assignments of the peaks we have done the two extreme hypothesis that the whole intensity corresponds to one assignment (this gives a maximum value for BR) or on the contrary that the whole intensity goes to the other assignment (leading to a minimum value for BR). The comparison between experiment and theory for the both excitation energies and beta-decay branching ratios is rather good. In particular, the prediction for the location of the 0^+, $T=2$ ^{28}P state is in excellent agreement with the experimental value. Also, the calculated half-life of 129 ± 18 ms (the error is due to the Q_{EC} uncertainty) is in excellent agreement with the measured value of 125 ± 10 ms.

Although possible, we have not yet calculated the spectroscopic factors for allowed proton decays of the 1^+ states to low-lying level in ^{27}Si.

We next comment on the more interesting results for the isospin-forbidden proton decay of the 0^+, $T=2$ state (^{28}P).

The isospin mixed wave function were calculated from the sd shell interaction of Wildenthal [28]) together with an empirical isospin nonconserving (INC) interaction derived in ref. [30]) on the basis of a least-squares fit to a selection of the experimentally measured b- and c-coefficients of the IMME. This INC interaction includes charge dependent and charge asymmetric terms in addition to the Coulomb term.

The 0^+ wave function can be calculated in the full proton-neutron space for all cases except ^{28}Si. Based on the calculated energies for ^{28}S, ^{28}P and ^{28}Mg, the predicted b and c coefficients of the IMME are 4700 and 218 keV, respectively. These are in reasonable agreement with the experimental values of 4804 and 214 keV (table 3). In the future we should also be able to make predictions for the d- and e-coefficients.

Since the ^{27}Si dimensions in the full proton-neutron space are on the order of 13 000, the model space for the present calculations had to be truncated. The dimensions were reduced to the order of 1500 by a truncation on the basis of the single-particle energies. The energies in this truncated basis are in good agreement

with experiment (see table 5) except for the ground state which is about 1 MeV too low theoretically. [The energies in the full space [28]) are all in good agreement with experiment. The defect in the truncated space is probably related to the "excitation-order convergence problem" discussed in ref. [31]).] The calculated spectroscopic factors (C^2S) and partial widths for the decay of the 0^+ $T=2$ state to low-lying levels in ^{27}Si are given in table 5. The penetration factors and single-particle widths were calculated with the usual prescription [32]) using 4.0 fm for the channel radius and $(3.85-E_x\ (\text{exp}))$ MeV for the Q-value.

The calculations correctly predict that the INC decay of the ^{28}P 0^+ $T=2$ state to the ^{27}Si first excited $\frac{1}{2}^+$ state should dominate. This is due both to the relatively large spectroscopic factor and to the $l=0$ rather than $l=2$ nature of this decay. The decays to the $\frac{5}{2}^+$ ground state and $\frac{3}{2}^+$ second excited states are predicted to be about a factor of 100 weaker, whereas the experiment indicates that they are only about a factor of 4 weaker. The not yet assigned 1.26 MeV proton peak can also be attributed to the 0^+ $T=2$ ^{28}P decay even if the calculated partial width is not favorable.

In ref. [33]) it was found that these isospin-forbidden decays are dominated by mixing with the nearby 0^+ states of lower isospin. The predicted 0^+ states ^{28}P below 8 MeV are at 0.72, 2.98, 3.54, 5.96 ($T=2$), 6.05, 7.06 and 7.30 MeV.

The closest $T=1$ state at 6.05 MeV could easily dominate the isospin-forbidden decay properties. However, the energies of these states are uncertain theoretically by at least 0.2 MeV [ref. [28])] and nothing is known experimentally. Perhaps the most that can be said theoretically is that one expects the isospin-forbidden spectroscopic

TABLE 5

Calculated spectroscopic factors and partial widths for the isospin forbidden decay of the ^{28}P 0^+, $T=2$ level to $T=\frac{1}{2}$ levels in ^{27}Si. Calculations are extended to ^{27}Si states beyond reach of the present experiment

J^π	E_x exp (MeV)	E_x theory (MeV) [a])	C^2S theory (10^{-3})	Partial width (keV)
$\frac{5}{2}^+$	0	−1.21	0.055	0.032
$\frac{1}{2}^+$	0.78	0.78	1.8	2.3
$\frac{3}{2}^+$	0.96	1.10	0.16	0.029
$\frac{5}{2}^+$	2.65	2.70	0.59	0.3×10^{-3}
$\frac{5}{2}^+$	2.86	2.61	7.0	2.4×10^{-3}
$\frac{1}{2}^+$	3.54	3.59	14.9	
$\frac{5}{2}^+$		3.89	2.9	
$\frac{3}{2}^+$	3.80	4.38	0.004	
$\frac{1}{2}^+$		5.33	14.2	

[a]) Adjusted to line up with the experimental 0.78 MeV state.

factors spread over a range of 0 up to about 0.01 and that the large spectroscopic factors may be associated with highly excited states in the final nucleus. On the other hand, the low-lying states with small spectroscopic factors often dominate simply because of the associated large Q-value and large penetration factors.

5. Summary

This paper reports on the first study of beta-delayed proton decay of ^{28}S ($T_z = -2$). This nucleus has been produced by projectile fragmentation of 85 MeV/u ^{36}Ar. The measured half-life of ^{28}S is 125 ± 10 ms. Energy spectra of beta-delayed protons have been measured and the lowest $T = 2, 0^+$ state in the daughter nucleus ^{28}P has been located at an excitation energy of 5900 ± 21 keV.

A comparison of the experimental data to the quadratic form of the isobaric multiplet mass equation shows that the energies of the five $T = 2$ states of the $A = 28$ quintet are well represented by that relation and shows no evidence for non-zero cubic and quartic term. A new mass-excess value of the ^{28}S ground state has been deduced from a now improved assumption of a purely quadratic IMME.

A partial ^{28}S decay scheme is proposed. Comparison with shell-model predictions shows an excellent agreement between experiment and theory for the half-life of ^{28}S and the location of the 0^+, $T = 2$ ^{28}P state and the b- and c-coefficients of the IMME. Concerning the branching ratios, ambiguities in the assignments of the peaks, lead to a more difficult comparison; nevertheless, theoretical and experimental values are compatible within the uncertainties. Calculations correctly predict that the isospin-forbidden proton decay of the 0^+, $T = 2$ ^{28}P state to the ^{27}Si first excited $\frac{1}{2}^+$ state should dominate. But the relative intensities of this state to the ^{27}Si (g.s.) and ^{27}Si (g.s) ($\frac{5}{2}^+$) are not well predicted. A better experimental knowledge of excited states in ^{28}P is really needed to go further.

To conclude, the experimental method described in the present paper is very powerful for the study of beta-delayed proton decay of neutron-deficient nuclei. This opens up the possibility for further studies, including gamma detection and proton–gamma coincidence detection which are needed to establish a complete decay scheme.

We would like to thank J. Vernotte and E. Kashy for fruitful discussion. We acknowledge the staff of the GANIL accelerator for the steady and intense ^{36}Ar beam. The technical assistance of A. Latimier, A. Richard and F. Geoffroy was of great importance for the success of this experiment. In particular we would also like to mention L. Stab and R. Bzyl who have manufactured our semi conductor telescope. We would like also to thank D. Grialou for the elaboration of this manuscript. This research was supported in part by the U.S. National Science Foundation under grant PHY 87-18772.

References

1) M. Langevin, A.C. Mueller, D. Guillemaud-Mueller, M.G. Saint-Laurent, R. Anne, M. Bernas, J. Galin, D. Guerreau, J.C. Jacmart, S.D. Hoath, F. Naulin, F. Pougheon, E. Quiniou and C. Détraz, Nucl. Phys. **A 455** (1986) 149
2) M.G. Saint-Laurent, J.P. Dufour, R. Anne, D. Bazin, V. Borrel, H. Delagrange, C. Détraz, D. Guillemaud-Mueller, F. Hubert, J.C. Jacmart, A.C. Mueller, F. Pougheon, M.S. Pravikoff and E. Roeckl, Phys. Rev. Lett. **59** (1987) 33
3) V. Borrel, J.C. Jacmart, F. Pougheon, A. Richard, R. Anne, D. Bazin, H. Delagrange, C. Détraz, D. Guillemaud-Mueller, A.C. Mueller, E. Rockel, M.G. Saint-Laurent, J.P. Dufour, F. Hubert and M.S. Pravikoff, Nucl. Phys. **A473** (1987) 331
4) E.P. Wigner, in Proc. Robert A. Welch Foundation Conf. on chemical research, Houston, 1957, ed. W.O. Milligan, vol. 1, p. 67
5) W. Benenson and E. Kashy, Rev. Mod. Phys. **51** no. 3 (1979) 527
6) M.S. Antony, J. Britz, J.B. Bueb and A. Pape, At. Data Nucl. Data Tables **33** (1985) 447; M.S. Antony, J. Britz, J.B. Bueb and V.B. Ndocko Ndongué, Nuovo Cimento **A88** (1985) 265
7) M.D. Cable, J. Honkanen, R.F. Parry, H.M. Thierens, J.M. Wouters, Z.Y. Zhou and J. Cerny, Phys. Rev. **C26** (1982) 1778
8) C.A. Gagliardi, D.R. Semon, E. Takada, D.M. Tanner and R.E. Tribble, Phys. Rev. **C37** (1988) 2889
9) A.G. Ledebuhr, Ph.D. Thesis, Michigan State University (1982) unpublished
10) R. Anne, D. Bazin, A.C. Mueller, J.C. Jacmart and M. Langevin, Nucl. Inst. Meth. **A257** (1987) 215
11) J.P. Dufour, R. Del Moral, H. Emmermann, F. Hubert, D. Jean, C. Poinot, M.S. Pravikoff, A. Fleury, H. Delagrange and K.H. Schmidt, Nucl. Instr. Meth. **A248** (1986) 267
12) A. Richard, private communication
13) J. Aysto, X.-J. Xu, D.M. Moltz, J.E. Reiff, J. Cerny and B.H. Wildenthal, Phys. Rev. **C32** (1985) 1700
14) P.M. Endt and C. Van der Leun, Nucl. Phys. **A310** (1978) 1
15) P.L. Reeder, A.M. Poskanzer, R.A. Esterlund and R. McPherson, Phys. Rev. **147** (1966) 781
16) A.H. Wapstra, G. Audi and R. Hoekstra, At. Data Nucl. Data Tables **39** (1988) 281
17) C.L. Morris, H.T. Fortune, L.C. Bland, R. Gilman, S.T. Greene, W.B. Cottinghane, D.B. Holtkamp, G.R. Burleson, C.F. Moore, Phys. Rev. **C25** (1982) 3218
18) G.R. Burleson, G.S. Blanpied, G.H. Daw, A.J. Viescas, C.L. Morris, H.A. Thiessan, S.J. Greene, W.J. Braithwaite, W. Cottingame, D.B. Holtkamp, I.B. Moore and C.F. Moore, Phys. Rev. **C22** (1980) 1180
19) C.J. Woodward, R.E. Tribble and D.M. Tanner, Phys. Rev. **C27** (1983) 27
20) K.A. Snover, D.W. Heikkinen, F. Riess, H.M. Kuan and S.S. Hanna, Phys. Rev. Lett. **22** (1969) 239
21) N.A. Jelley, N. Anyas-Weiss, M.R. Wormald, B.Y. Underwood and K.W. Allen, Phys. Lett. **B40** (1972) 200
22) D.F.H. Start, N.A. Jelley, J. Burde, D.A. Hutcheon, W.L. Randolph, B.Y. Underwood and R.E. Warner, Nucl. Phys. **A206** (1973) 207
23) J.L. Olsen and G.D. O'Kelley, Phys. Rev. **93** (1954) 1125
24) G. Audi, W.G. Davies and G.E. Lee-Whiting, Nucl. Instr. Meth. **A249** (1986) 443
25) J. Äystö, M.D. Cable, R.F. Parry, J.M. Wouters, D.M. Moltz and Joseph Cerny, Phys. Rev. **C23** (1981) 879
26) A.G. Ledebuhr, L.H. Harwood, R.G.H. Robertson and T.J. Bowles, Phys. Rev. **C22** (1980) 1723
27) B.D. Anderson *et al.*, private communication
28) B.H. Wildenthal, Prog. Part. Nucl. Phys. **11** (1984) 5
29) B.A. Brown and B.H. Wildenthal, At. Data Nucl. Data Tables **33** (1985) 347
30) W.E. Ormand and B.A. Brown, Nucl. Phys. **A440** (1985) 274; **A491** (1989) 1
31) B.A. Brown and B.H. Wildenthal, Ann. Rev. Nucl. Part. Sci. **38** (1988) 29
32) D. Mikolas, B.A. Brown, W. Benenson, L.H. Harwood, E. Kashy, J.A. Nolen, B. Sherrill, J. Stevenson, J.S. Winfield, Z.-Q. Xie and R. Sherr, Phys. Rev. **C37** (1988) 766
33) W.E. Ormand and B.A. Brown, Phys. Lett. **B174** (1986) 128